# Specific ion effects in polysaccharide dispersions

Contents lists available at ScienceDirect

Carbohydrate Polymers

journal homepage: www.elsevier.com

# Specific ion effects in polysaccharide dispersions

Duccio Tatini[a], Filippo Sarri[a], Piefrancesco Maltoni[a], Moira Ambrosi[a], Emiliano Carretti[a], Barry W. Ninham[a, b], Pierandrea Lo Nostro[a, *]

[a] Department of Chemistry Ugo Schiff and CSGI, University of Florence, 50019 Sesto Fiorentino, Firenze, Italy
[b] Department of Applied Mathematics, Research School of Physical Sciences and Engineering, Australian National University, Canberra, ACT 2600, Australia

ARTICLE INFO

*Article history:*
Received 17 March 2017
Received in revised form 22 May 2017
Accepted 24 May 2017
Available online xxx

*Keywords:*
Polysaccharide(s)
Guar gum
Sodium hyaluronate
Specific ion effect
Viscosity
Thermal properties

ABSTRACT

The specific effects induced by some strong electrolytes or neutral cosolutes on aqueous mixtures of guar gum (GG), sodium alginate (SA) and sodium hyaluronate (SH) were studied through rheology and DSC experiments. The results are discussed in terms of changes in the polymer conformation, structure of the network and hydration properties. This study is also aimed at controlling the viscosity of the aqueous mixturesfor application in green formulations to be used as fracturing fluids for shale gas extraction plants.



## 1. Introduction

Hofmeister, or specific ion effects consist in changes induced in a measurable phenomenon or physico-chemical property by the addition of a specific salt. These effects usually take place at moderately high concentrations, e.g. above 10 mM. They occur in a large variety of systems and practically in all realms of nature: in bulk solutions, aqueous and non-aqueous systems, at interfaces and in self-assembled structures (Lo Nostro & Ninham, 2012; Lo Nostro & Ninham, 2016).

Compared to the pristine sequence found by Hofmeister in his studies on the precipitation of albumin dispersions, other systems may exhibit a different order. However, in general it is observed that as the ion changes, the measured properties are affected. Recently it has been found that the charge and polarity of the involved species and surfaces are crucial factors in determining whether the effectiveness of the salts follows the direct or reverse Hofmeister series (Schwierz, Horinek, Sivan, & Netz, 2016). In a dilute regime, electrostatics dominates the picture of ionic interactions, and Coulomb potential describes the behavior of the solution, with a substantial correct prediction of the ionic activity coefficient. However, electrostatic interactions are non ion-specific, while the surface charge density depends on the ion size. At high salt concentrations, non-electrostatic forces come into play, Coulomb interactions are screened, and ion specificity emerges.

The rheology and thermal behaviors of solutions and dispersions of biopolymers such as polysaccharides are examples of specific ion effects, in fact such features can be tuned by the proper choice of electrolytes at a suitable concentration. This topic has been fully investigated in the literature (see Hatakeyama, Tanaka, & Hatakeyama, 2010; Guan, Xu, & Huang, 2010; Kupská, Lapcík, Lapcíková, Záková, & Juríková, 2014, and references therein). One of the more interesting insights is the mechanism through which such effects take place. Norton studied the disorder-order transition and the helix–helix aggregation in κ-carrageenan in the presence of different salts, and concluded that these phenomena depend on the salt-induced modification of the solvent quality of water, and not on direct salt-polyelectrolyte interactions (Norton, Morris, & Rees, 1984). Along the same line, Xu explained the effect of salts on the sol-gel transition of methylcellulose in terms of the ability of individual ions to change water structure and of the strength of the interactions between water molecules (Xu, Wang, Tam, & Li, 2004).

As a final point regarding the application of the above theoretical model to salting-in and salting-out phenomena, we return to the fact that, in general, the surface of a macromolecule exposes sites (functional groups) which differ in their relative affinities to the components of the mixed solvent. (Piculell & Nilsson, 1989).

A more relevant study is that by Yin on the gelation of konjac glucomannan (KGM) and in particular on its rheological behavior in the presence of different salts. The increase in the viscosity upon addition of salting-out salts is explained in terms of (i) the modification of the water structure or (ii) by the change in the interactions between the ions and specific sites on the polymer chains (Yin, Zhang, Huang, &

* Corresponding author at: Department of Chemistry Ugo Schiff, Via della Lastruccia 3, 50019 Sesto Fiorentino, Firenze, Italy.
*Email addresses:* duccio.tatini@unifi.it (D. Tatini); filippo.sarri@unifi.it (F. Sarri); pierfrancesco.maltoni@stud.unifi.it (P. Maltoni); moira.ambrosi@unifi.it (M. Ambrosi); emiliano.carretti@unifi.it (E. Carretti); barry.ninham@anu.edu.au (B.W. Ninham); pierandrea.lonostro@unifi.it (P. Lo Nostro)

http://dx.doi.org/10.1016/j.carbpol.2017.05.078
0144-8617/

Nishinari, 2008). Finally, Singh investigated the gelling behaviour of agarose with $Na_2SO_4$, and found that the release of water from the gel is due to the water withdrawing action of sulfate ions (Singh, Meena, & Kumar, 2009).

In the present contribution we report a study on the effect induced by some strong electrolytes and neutral cosolutes on the rheology and thermal behavior of some polysaccharide aqueous dispersions and solutions. The results are discussed in terms of the Hofmeister series, ion-polymer and polymer-water interactions.

This investigation is relevant for the application of polysaccharides in green formulations for fracturing fluids used in shale gas extraction (Barati & Liang, 2014; Kelly, Khan, Leduc, Tayal, & Prud'homme, 2001; Legemah, Qu, Sun, Beall, & Zhou, 2013).

The basic ingredients that are commonly used in fracturing fluids comprise water, more or less chemically modified polysaccharides as gelling agents (guar gum, cellulose, xanthan gum and their derivatives), a large number of salts as formulation stabilizers or clay control agents, acids (e.g. HCl, $H_3BO_3$ and citric acid) and bases to adjust the pH, cross-linker initiators (potassium borate or metaborate, complexes of zirconium or titanium with organic chelators), naphtha derivatives and surfactants (Barati & Liang, 2014; Gandossi & Von Estorff, 2015; Li, Al-Muntasheri, & Liang, 2016; Montgomery 2013).

Several scientists have discussed a number of possible environmental risks related to the production of shale gas. These include the accidental release of fracturing fluids, leaks of hydrocarbons, the uptake of Naturally Occurring Radioactive Materials (NORM), the introduction of foreign bacterial strains to the sub-surface, and induced micro-seismicity (Arthur, Bohm, Coughlin, Layne, & Cornue, 2009; Holloway & Rudd, 2013, Chapter 11; Osborn, Vengosh, Warner, & Jackson, 2011; Vengosh, Jackson, Warner, Darrah, & Kondash, 2014). To limit some of these risks, we focus on "greener" formulations, which employ biocompatible and non-toxic ingredients.

## 2. Hypotheses

This study is aimed at demonstrating that the thermal and rheological properties of aqueous mixtures containing guar gum, sodium alginate and sodium hyaluronate can be significantly modified by using strong electrolytes, and that salt specific effects show up, following the Hofmeister series. The ions exhibit particular effects related to their structure and particularly to their capability to interfere with the polymer hydrogen bonding network and with the solvent properties of water. The results support our effort to formulate green alternatives to the currently used hydraulic fracturing fluids.

## 3. Experimental

### 3.1. Materials

All chemicals were reagent grade (≥99%) and used as received. NaF, NaI, NaSCN, $NaClO_4 \cdot H_2O$, $NaH_2PO_4$ were purchased from Fluka (Milan, Italy). NaCl, NaBr, $Na_2SO_4$, $Na_3PO_4 \cdot 3H_2O$, $Na_2HPO_4 \cdot 7H_2O$, trehalose and sodium alginate (average molecular mass 240 kDa; mannuronate/guluronate ratio 0.44) were supplied by Sigma-Aldrich (Milan, Italy). Urea was purchased from Riedel de Haen (Germany). Guar gum (average molecular mass 2000 kDa) was supplied by Lamberti S.p.A. (Milan, Italy); high molecular weight (1800–2000 kDa) sodium hyaluronate was purchased from Stanford Chemicals Company (Fairbanks, CA). All solutions and dispersions were prepared with bidistilled Milli-Q water (resistivity >18 MΩ·cm at 25 °C).

### 3.2. Sample preparation

In general gelling agents for fracturing formulations are used up to 1% w/w (Couillet & Hughes, 2008; Kelly et al., 2001). The addition of a crosslinker lowers the concentration to 0.1–0.5% (Goel, Shah, & Grady, 2002). We chose a polysaccharide concentration of 1% to avoid the addition of a crosslinker; in this way we can focus exclusively on the effect of the salt on the polymer chains.

GG, SA and SH 1% w/w water mixtures were prepared by slowly adding a weighted amount of polysaccharide powder to water under constant stirring at room temperature. In these conditions complete dissolution occurs in about one hour for all the investigated biopolymers. The samples containing the different salts or co-solutes were prepared following the same procedure, replacing water with 0.5 M aqueous solutions of the salts or neutral co-solutes.

### 3.3. Rheology

Rheological measurements were performed on a Paar Physica UDS 200 rheometer working in the controlled shear-stress mode. For all samples a plate–plate geometry (diameter, 2.5 cm; gap, 300 μm) was used. Under these conditions the total amount of the sample in the cell was about 0.4 mL. All measurements were performed at 25.0 °C (Peltier control system). For each sample the flow curve was acquired in a torque range between $10^{-3}$ and 2000 mN m, after a 15 min soaking time to equilibrate at the set temperature.

### 3.4. Thermal properties

Differential Scanning Calorimetry (DSC) was performed by means of a DSC-Q2000 by TA Instruments (Philadelphia, PA). The samples were first cooled from 20° to −60 °C at 10 °C/min, then heated up to 50 °C at 5 °C/min. Measurements were conducted in $N_2$ atmosphere, with a flow rate of 50 mL/min. For the samples prepared with NaF and $Na_2HPO_4$ the deconvolution of endothermic peaks was performed by means of the Igor Pro 6.36 software, using a summation of exponentially modified Gaussian (EMG) functions (Tatini et al., 2015). The single EMG function is defined as:

$$f(T) = \sqrt{\frac{\pi}{2}} \frac{hw}{|s|} \exp\left[\frac{w^2}{2s^2}\left(\frac{T_0 - T}{s}\right)\right] \operatorname{erf}\left[\frac{T_0 - T}{2\left(w + \frac{w}{|s|}\right)}\right]$$

where $h$ is the height, $T_0$ the center, $w$ the width of the peak and $s$ is the distortion factor (shape). For the deconvoluted peaks, the peak temperatures correspond to $T_0$, while the enthalpy changes are calculated using the total area under the peak.

## 4. Results and discussion

The thermal and rheological properties of the investigated polysaccharides were studied in their pure aqueous mixtures and after the addition of some sodium salts or neutral cosolutes (trehalose and urea). It may sound trivial, but it is important to underline that in the two experimental techniques used in this study the sample is treated in totally different manners. In DSC the specimen remains still and is heated/cooled above and below room temperature. On the other hand, during the acquisition of the flow curve the sample is mechanically stressed at constant temperature, its supramolecular texture is modi-

fied and its reaction to this perturbation recorded. The thermal behavior (studied through DSC) reflects the interactions between the cosolutes, the polymer chains and water; while the rheological behavior depends on the interactions between the polymer chains, and their distribution and entanglement in the matrix.

### 4.1. Thermal behavior

The thermograms of 1% aqueous mixtures of GG, SA and SH are reported in Fig. 1.

The endothermic peak, due to the melting of free water, is always centered slightly above 0 °C, presumably because of a kinetic effect (Hatakeyama et al., 2010; Naoi, Hatakeyama, & Hatakeyama, 2002). The melting peak temperatures ($T_{mf}$) and the corresponding enthalpy changes ($\Delta H_{mf}$, in J/g) are listed in Table 1. GG shows the highest melting temperature, associated to the lowest melting enthalpy, while SH possesses the lowest peak temperature and the largest melting enthalpy. SA shows intermediate values.

The thermograms of GG in the presence of different 0.5 M solutions of sodium halides are shown in Fig. 2.

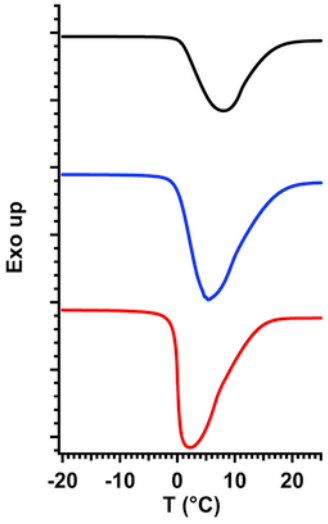


**Fig. 1.** DSC heating curves of 1% aqueous mixtures of GG (black), SA (blue), and SH (red). Curves have been offset for graphical purposes. (For interpretation of the references to colour in this figure legend, the reader is referred to the web version of this article.)

In the case of NaF the endothermic peak shows a bimodal behavior. The curve was deconvoluted by using an exponentially modified Gaussian function (EMG) according to Eq. (1). This approach is commonly implemented in the analysis of overlapping DSC peaks in drugs (Elsabee & Prankerd, 1992), paraffins (Anghel, Georgiev, Petrescu, Popov, & Constantinescu, 2014) and polymer composites characterization (Tatini et al., 2015). The fitting procedure provides the two $T_0$ values corresponding to the centers of the two Gaussian curves used for the deconvolution. $T_0$ are found to be 5.07 and −4.45 °C. This bimodal behavior is increased with increasing halide atomic number: in the case of NaCl, NaBr and NaI two distinct peaks appear in the DSC curve whose distance increases moving down in the group. The higher temperature peak corresponds to the melting of free water ($T_{mf}$ in Table 1) and is similar to the peak produced by the salt-free GG dispersion. The lower temperature peak located between −30 and −5 °C relates to the melting of freezable bound water ($T_{mb}$ in Table 1), that freezes below 0 °C and has a reduced enthalpy of fusion (Chaplin, 2012).

For the samples containing pure GG, SA and SH the peak related to the melting of freezable bound water is not observed. Presumably the freezable bound and the free water melting peaks overlap together in the broad endothermic signal which is centered around 0 °C in the heating scans (see Fig. 1). A similar behavior was reported by Nakamura in the case of cellulose with different amounts of adsorbed water (Nakamura et al., 1981). The addition of a salt modifies the interactions between water and the polysaccharide chains, and changes the distribution of water between the two states: freezable bound and free water. This effect induces a separation of the two overlapping peaks, which is strictly dependent on the salt nature.

The melting point and the enthalpy change for the bound freezable water depend on the interactions between the polymer chains and water (Guan et al., 2011).

As proposed by De Andres-Santos for 1% aqueous solutions of sodium hyaluronate, we assume that the lower $T_{mb}$, the higher the number of water and polysaccharide molecules that remain closely associated to each other, i.e., the more hydrated the chains (De Andres-Santos, Velasco-Martin, Hernández-Velasco, Martín-Gil, & Martín-Gil, 1994). On the other hand, a higher $T_{mb}$ indicates an increment in the interchain hydrogen bonding (HB) interactions within the polysaccharide, thus suggesting a sort of de-hydration of the polymer.

The results obtained for the samples containing the sodium halides show no remarkable variation in $T_{mf}$ and $\Delta H_{mf}$ with the exception of NaF. Instead, the values of $T_{mb}$ decrease from −4.45 (NaF) to −29.65 °C (NaI), while $\Delta H_{mb}$ decreases from 125.8 (NaF) to

**Table 1**
Melting temperature and enthalpy change of free water ($T_{mf}$ and $\Delta H_{mf}$, in °C and J/g) and of the freezable bound water ($T_{mb}$ and $\Delta H_{mb}$, in °C and J/g) in 1% aqueous mixtures of guar gum, sodium alginate, and sodium hyaluronate, in the presence of different salts or neutral cosolutes. The concentration of all cosolutes is always 0.5 M, unless otherwise specified.

| additive | $T_{mf}$ | $\Delta H_{mf}$ | $T_{mb}$ | $\Delta H_{mb}$ | $T_{mf}$ | $\Delta H_{mf}$ | $T_{mb}$ | $\Delta H_{mb}$ | $T_{mf}$ | $\Delta H_{mf}$ | $T_{mb}$ | $\Delta H_{mb}$ |
|---|---|---|---|---|---|---|---|---|---|---|---|---|
| Guar Gum 1% | | | | | Sodium Alginate 1% | | | | Sodium Hyaluronate 1% | | | |
| none | 7.88 | 307.3 | | | 5.36 | 336.4 | | | 2.18 | 353.0 | | |
| NaF | 5.07 | 155.5 | −4.45 | 125.8 | 1.16 | 273.7 | −4.11 | 56.39 | 0.66 | 300.8 | −5.23 | 40.46 |
| NaCl | 1.05 | 245.2 | −19.98 | 22.11 | 1.33 | 241.8 | −19.82 | 21.50 | −0.03 | 260.1 | −20.43 | 23.77 |
| NaBr | 1.80 | 249.7 | −26.03 | 16.58 | 0.05 | 267.3 | −26.34 | 17.78 | −0.16 | 268.8 | −26.71 | 19.18 |
| NaI | 1.62 | 256.2 | −29.65 | 15.07 | 0.07 | 267.6 | −29.73 | 16.40 | −0.57 | 272.4 | −29.99 | 16.54 |
| $Na_2SO_4$ | 4.24 | 318.4 | | | 2.61 | 334.1 | | | 2.49 | 331.8 | | |
| NaSCN | 1.54 | 282.7 | | | −0.22 | 276.3 | | | −0.13 | 289.4 | | |
| $NaClO_4$ | 2.58 | 278.2 | | | −0.35 | 293.6 | −33.23 | 12.28 | −0.22 | 299.6 | −33.19 | 5.678 |
| $Na_3PO_4$ | 1.28 | 58.88 | | | 4.42 | 294.8 | | | 0.64 | 317.6 | | |
| $Na_2HPO_4$ | 5.13 | 293.5 | | | 1.50 | 331.9 | | | 1.79 | 274.5 | | |
| $NaH_2PO_4$ | 3.00 | 291.5 | | | −0.23 | 295.8 | | | −0.32 | 307.5 | | |
| Urea | 3.48 | 247.9 | −10.62 | 8.342 | 2.03 | 254.1 | −11.11 | 11.68 | 0.00 | 268.8 | −11.83 | 13.67 |
| Trehalose | 1.56 | 255.2 | | | 0.59 | 279.9 | | | 0.07 | 261.9 | | |

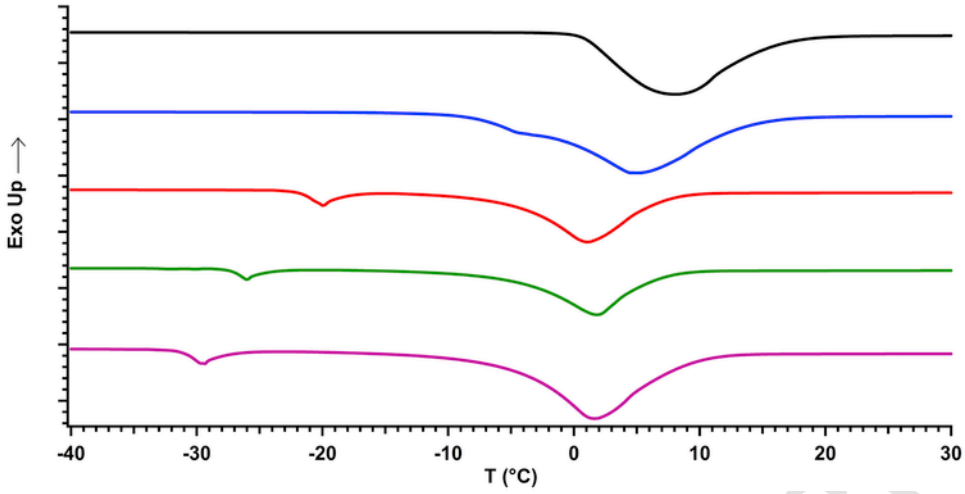


**Fig. 2.** DSC heating curves of 1% aqueous mixtures of GG pure (black) and in the presence of 0.5 M solutions of NaF (blue), NaCl (red), NaBr (green) and NaI (magenta). Curves have been offset for graphical purposes. (For interpretation of the references to colour in this figure legend, the reader is referred to the web version of this article.)

15.07 J/g (NaI). These trends suggest the presence of a specific anion effect on the conformational structure and intermolecular interactions of GG. In particular, the more chaotropic the anion, the lower the value of $T_{mb}$ and hence the lower the number of interacting sites between the polysaccharide chains. We argue that strongly hydrated kosmotropic anions like fluoride and sulfate compete with the polysaccharide chains for water molecules, thus lowering the hydration of the chains (Yin et al., 2008). This effect promotes the formation of interchain HB and eventually leads to the aggregation of polysaccharide molecules.

On the other hand, the presence of chaotropic anions, like iodide, modifies the dimensions of the polysaccharide coils and increases their solvent-accessible surface area (ASA) (Curtis, Steinbrecher, Heinemann, Blanch, & Prausnitz, 2002). These ion hydration effects that lead to the salting-in processes induced by chaotropes and salting-out by kosmotropes on proteins has been extensively studied (López-Arenas, Solís-Mendiola, Padilla-Zúñiga, & Hernández-Arana, 2006). The ruling mechanism by which chaotropes increase the solvation of the polymer surface seems to be a direct interaction of the ions with the weakly hydrated portions of the polysaccharide chain, as already found and reported in the case of proteins (Arakawa & Timasheff, 1982; Collins, 2004; Lo Nostro & Ninham, 2012).

The presence of urea produces a second endothermic peak in the thermogram, related to the melting of freezable bound water. At this concentration urea usually acts as an enhancer of the solvation of the polysaccharide chains (Winkworth-Smith, MacNaughtan, & Foster, 2016) by promoting their unfolding.

In the case of the other additives ($Na_2SO_4$, NaSCN, $NaClO_4$, $Na_3PO_4$, $Na_2HPO_4$, $NaH_2PO_4$ and trehalose) only a broad endothermic peak around 0 °C is clearly detected (see Table 1, and Figs. S1 and S2 in Supplementary material). The presence of these cosolutes does not induce a separation between the freezable bound and the free water melting peaks, resulting in a DSC profile which is similar to those of pure GG, SA and SH samples (Fig. 1). The case of $Na_2SO_4$ is peculiar as it shows a value of $\Delta H_{mf}$ (318.4 J/g) which is close to that of pure water (333.5 J/g). The sulfate ions strongly interact with the water molecules inducing a de-hydration of the polysaccharide chains, reducing the amount of freezable bound water in favour of the free water, and resulting in an overlap of the two DSC signals.

The effect induced by $Na_2HPO_4$ is peculiar and deserves an in-depth analysis. The DSC curve (Fig. S3 in Supplementary material) shows a shoulder at about 20 °C. This phenomenon can be related to a liquid crystalline-to-isotropic liquid state transition (Hatakeyama, Naoi, & Hatakeyama, 2004; Nakamura, Hatakeyama, & Hatakeyama, 1991). Since this transition is observed both for GG and SA samples, we argue that the presence of $Na_2HPO_4$ preserves the liquid crystalline phase in the guar and sodium alginate network, whereas all the other examined salts and co-solutes destabilize this state.

In order to separate the two endothermic contributions and calculate the enthalpy for this transition, EMG deconvolution was performed and the fitting parameters ($T_{ph}$ and $\Delta H_{ph}$) are shown in Table S1 (see the Supplementary material). For GG the liquid crystalline-to-isotropic liquid state transition occurs at $T_{ph}$ = 19.3° C, with a corresponding enthalpy change of 24.68 J/g.

Aqueous solutions of SA and SH in the presence of salts and cosolutes show an identical thermal behavior to that previously described for GG dispersions. The values of $T_{mf}$, $\Delta H_{mf}$, $T_{mb}$ and $\Delta H_{mb}$ extracted from the thermograms are reported in Table 1. SH and SA samples show analogous DSC curves to the corresponding GG samples, with the exception of perchlorate. For both SA and SH systems, the thermograms of perchlorate containing sample shows two peaks instead of one, as in the GG/perchlorate sample. An extra peak appears at about −33 °C and can be ascribed to the freezable bound water melting. This peak may reflect polymer-salt interactions similar to those occurring with other chaotropic ions. In the GG sample this peak is not shown, indicating that a different mechanism occurs. It is worthwhile to mention that $ClO_4^-$ may act as an oxidizer and it is extensively used as gel breaker in guar-based formulations (Hall, Szemenyei, & Gupta, 1991; Schnoor, Singh, & Russel, 2016; Schultheiss, 2015). Presumably perchlorate partially oxidizes the polysaccharide chains, inducing a structural modification and a change in the polymer-water interactions, and the peak for the melting of freezing bound water disappears. This mechanism does not take place with the partially anionic chains of SA and SH.

### *4.2. Rheology*

#### *4.2.1. Fitting of the flow curves*

All the flow curves show a similar profile (see Fig. 3). At low shear rate all mixtures exhibit a Newtonian plateau. For stronger perturbations a shear thinning region is shown.

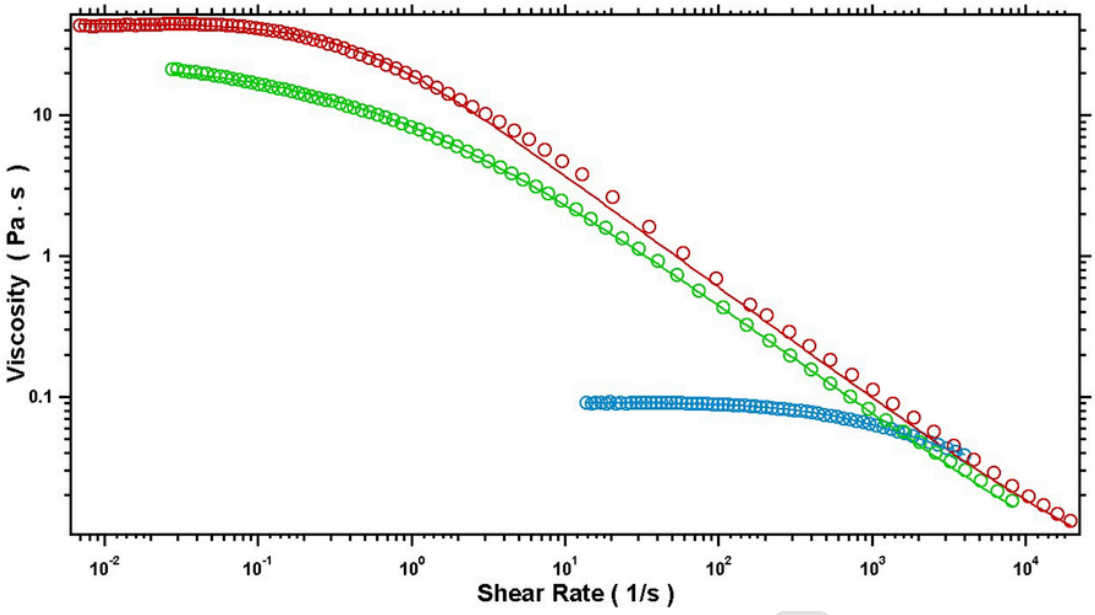


**Fig. 3.** Flow curves for 1% w/w SA (light blue), GG (green), and SH mixtures (red). The solid lines represent the fitting of the experimental curves. (For interpretation of the references to colour in this figure legend, the reader is referred to the web version of this article.)

We applied the Bird–Carreau–Yasuda (BCY) rheological model to the flow curves. This model, sometimes referred to as Carreau–Yasuda or Carreau model (Barnes, Hutton, & Walters, 1989), was empirically developed to describe the mechanical behavior of systems that exhibit both a Newtonian and a shear thinning region (Osswald & Rudolph, 2015). In particular it is used to study the rheology of polymeric water-based dispersions and solutions, e.g. those from polyacrylamide (Escudier et al., 2005), polypropylene (Lertwimolnun & Vergnes, 2006), and polysaccharides such as SH (Haward, Jaishankar, Oliveira, Alves, & McKinley, 2013), GG (Nandhini Venugopal & Abhilash, 2010), xanthan gum and carboxymethylcellulose (Escudier, Gouldson, Pereira, Pinho, & Poole, 2001; Escudier et al., 2005; García, Alfaro, Calero, & Muñoz, 2014).

In the BCY model the following equation describes the dependence of the viscosity value η:

$$\eta = \eta_\infty + \left(\eta_0 - \eta_\infty\right) \cdot [1 + (\lambda\dot{\gamma})^a]^{(n-1)/a} \quad (2)$$

where $\eta$, $\eta_0$, $\eta_\infty$, $\dot{\gamma}$, $\lambda$, $n$, and $a$ are the viscosity, the zero shear rate viscosity, the viscosity at infinite shear, the applied shear rate, the yield of shear rate above which the system shows a shear thinning behavior, the power law index, and the Yasuda parameter indicating the width of the transition region between $\eta_0$ and $\eta_\infty$, respectively (Carreau, 1972; Osswald & Rudolph, 2015; Yasuda, Armstrong, & Cohen, 1981).

Almost all flow curves containing GG and SH are well fitted (as shown by the $\chi^2$, see Table 2) by the BCY model with the sole exceptions of SH in the presence of $Na_3PO_4$ and of the SA solutions, which show a very low variability in the whole shear range examined. Table 2 lists the values of $\boldsymbol{\eta}_0$, $\boldsymbol{\lambda}$, $a$ and $n$ extracted from the fitting of the flow curves, according to Eq. (2).

*4.2.2. Flow curves*

In order to check the effect of different salts on the viscosity of polysaccharide mixtures, we mainly focussed our attention on the trend of $\eta_0$ value.

**Table 2**
The zero shear rate viscosity ($\eta_0$, in Pa s), power law index ($n$), the reciprocal of the critical shear rate at which the viscosity begins to drop down (λ, in s), the width of the transition region between $\eta_0$ and $\eta_\infty$ ($a$), and the $\chi^2$ extracted from the fitting of the flow curves for 1% aqueous mixtures of guar gum and sodium hyaluronate, in the presence of different salts or neutral cosolutes. The concentration of all cosolutes is always 0.5 M, unless otherwise specified.

| additive | $\eta_0 \pm 2.5\%$ | n ± 4% | λ ± 5% | a ± 3% | $\chi^2$ | $\eta_0 \pm 1.5\%$ | n ± 15% | λ ± 9% | a ± 4% | $\chi^2$ |
|---|---|---|---|---|---|---|---|---|---|---|
| Guar Gum 1% | | | | | | Sodium Hyaluronate 1% | | | | |
| none | 24.41 | 0.20 | 1.36 | 0.58 | 6.96 | 44.66 | 0.20 | 2.22 | 1.21 | 51.71 |
| NaF | 33.30 | 0.19 | 1.64 | 0.65 | 13.29 | 28.05 | 0.19 | 0.87 | 0.57 | 7.12 |
| NaCl | 25.23 | 0.22 | 1.19 | 0.58 | 7.28 | 44.84 | 0.21 | 2.14 | 1.00 | 72.92 |
| NaBr | 23.68 | 0.22 | 1.24 | 0.57 | 3.64 | 40.95 | 0.26 | 2.07 | 0.93 | 98.98 |
| NaI | 19.70 | 0.24 | 1.11 | 0.51 | 6.88 | 46.23 | 0.15 | 1.22 | 0.55 | 6.25 |
| $Na_2SO_4$ | 43.53 | 0.21 | 3.14 | 0.67 | 32.67 | 21.01 | 0.22 | 0.76 | 0.59 | 3.75 |
| NaSCN | 28.27 | 0.16 | 1.12 | 0.42 | 7.05 | 40.96 | 0.27 | 2.11 | 0.68 | 39.50 |
| $NaClO_4$ | 23.87 | 0.22 | 1.47 | 0.67 | 10.10 | 53.09 | 0.28 | 2.93 | 0.84 | 32.18 |
| $Na_2HPO_4$ | 30.07 | 0.20 | 2.02 | 0.80 | 16.01 | 77.68 | 0.22 | 2.58 | 1.18 | 26.14 |
| $NaH_2PO_4$ | 20.44 | 0.19 | 1.01 | 0.63 | 3.50 | 19.75 | 0.30 | 1.22 | 0.70 | 12.07 |
| $Na_3PO_4$ | 19.90 | 0.24 | 1.29 | 0.64 | 5.36 | | | | | |
| Urea | 33.68 | 0.23 | 2.16 | 0.66 | 10.45 | 46.21 | 0.26 | 1.98 | 0.78 | 3.83 |
| Trehalose | 37.65 | 0.21 | 2.60 | 0.66 | 38.32 | 159.25 | 0.20 | 6.07 | 0.90 | 73.50 |

Fig. 3 shows the flow curves for the 1% aqueous mixtures of SA, GG and SH. All samples exhibit a specific non-Newtonian behavior: the zero shear viscosity of SH and GG water-based systems are in the order of tens of Pa s ($\eta_0$ = 44.66 and 24.41 Pa s, respectively), while the alginate system shows a low value, about 0.11 Pa s in the whole explored torque range. On the other hand, the addition of salts or neutral co-solutes induces remarkable changes in the rheological properties of GG and SH (see Table 2).

Fig. 4 illustrates the effect of trehalose, $Na_2SO_4$ and NaF on the profile of the flow curve of SH and GG. For SH the presence of trehalose led to an increase of the strength of the tridimensional network, as indicated by the increase of $\eta_0$ (from 44.66 up to 159.25 Pa s) and by a shift of the yield value of $\dot{\gamma}$, $\lambda$. On the other hand, sulfate and fluoride lower both the $\eta_0$ (21.01 and 28.05 Pa s respectively) and the $\lambda$ values.

A similar trend is obtained for trehalose and GG, while the addition of $Na_2SO_4$ and NaF to GG induces an opposite effect, as indicated by the raise in the zero shear viscosity (from 24.41 up to 43.53 and 33.30 Pa s, respectively), and by the shift of $\lambda$ to higher values. These results suggest a synergistic interaction between trehalose and the polysaccharide molecules, which is more significant for SH. We argue that trehalose establishes crosslinking intra- and intermolecular interactions, resulting in a strengthening of the system.

Indeed, trehalose is known as a kosmotrope or water-structure maker: this disaccharide is able to break the tetrahedral HB network of water and re-order the water molecules in the hydration layer (Branca et al., 2005; Lerbret et al., 2005). However, experiments conducted by us on a 0.5 M solution of trehalose in water show neither an increase in the viscosity, nor a modification in the rheological response.



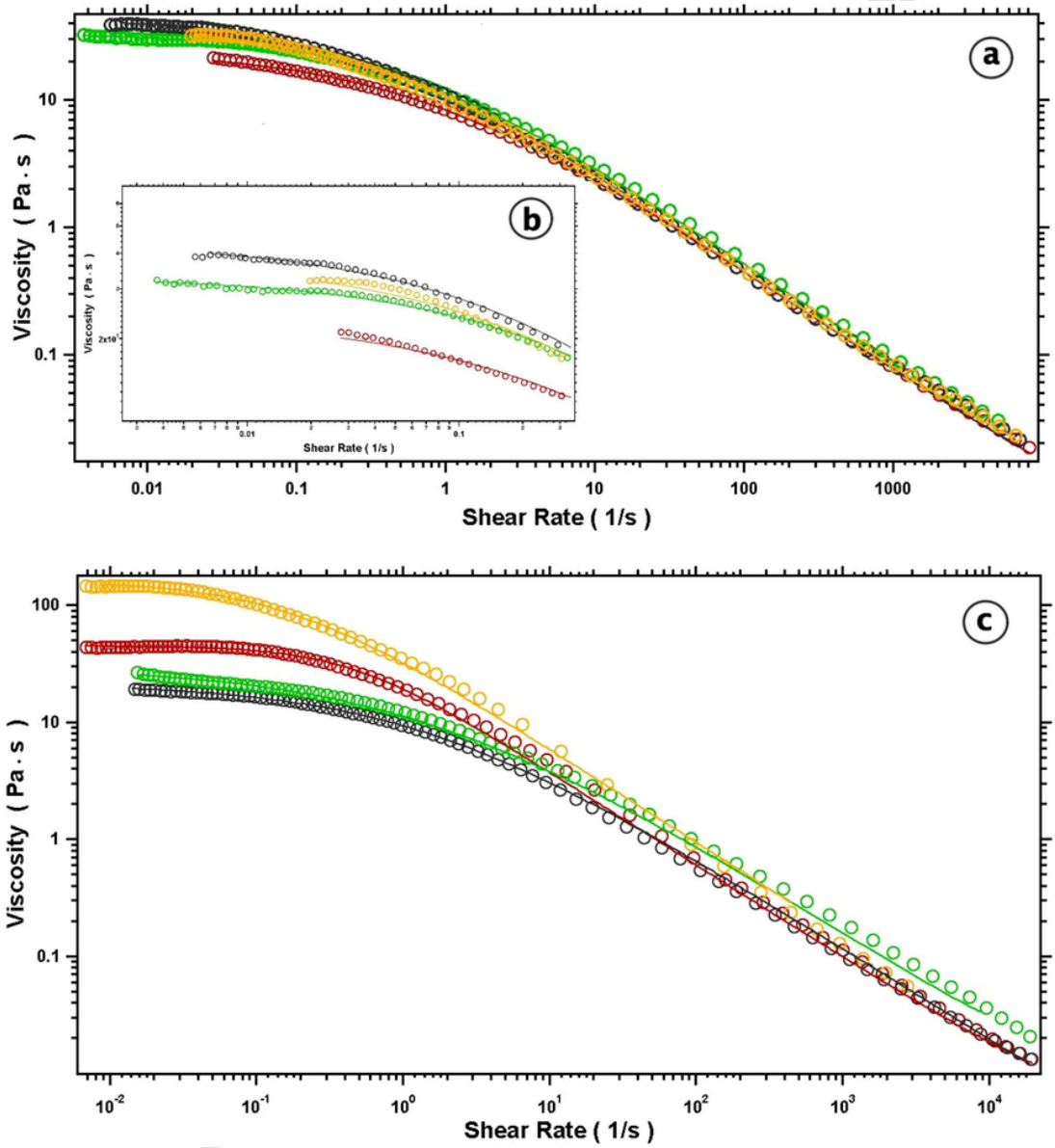


**Fig. 4.** Flow curves of (a) GG and SH (c) 1% w/w mixtures (red) and in the presence of 0.5 M trehalose (yellow), NaF (green) and $Na_2SO_4$ (grey). The inset (b) shows the flow curves of GG zoomed at low shear stress. The solid lines represent the fitting of the experimental curves. (For interpretation of the references to colour in this figure legend, the reader is referred to the web version of this article.)

The competition for water molecules between trehalose and the polysaccharide chains leads to partial de-hydration of the macromolecules (Jain & Roy 2008). It has been shown that trehalose can modify the hydration layer of biomolecules (Kawai, Sakurai, Inoue, Chujo, & Kobayashi, 1992; Magazù, Migliardo, Musolino, & Sciortino, 1997), stabilizing their HB network. This picture, commonly known as *preferential exclusion theory*. The *water replacement theory* instead argues that the hydration layer of the macromolecules is substituted by trehalose, which directly forms HB and stabilizes the structure. A third approach, the *vitrification theory*, can be applied only at higher concentration of trehalose and envisages that it creates a glassy matrix which acts as a protective cocoon, shielding and stabilizing the macromolecules from external stresses (Jain & Roy 2008). Since in our case the concentration of trehalose is relatively low, we can exclude the latter hypothesis. In the case of sulphate we propose two different mechanisms, depending on the investigated polysaccharide. The $SO_4^{2-}$ ion is a kosmotrope, which subtracts water from the macromolecule hydration layer. In the case of SH, where negatively charged $-COO^-$ groups are distributed along the chains, the addition of sulfate brings about a weakening in the polymeric network, that results in a decrease of the strength of the polymeric network. Conversely for GG the reduction of water molecules in the hydration layer promotes the formation of interchain interactions, due to the non-ionic nature of the polysaccharide. Therefore, the strength of the polymeric network increases, as indicated by the trend of both the viscosity and the $\lambda$ values.

Moreover, also the effect of fluoride supports this argument. Indeed, kosmotropic ions like fluoride and sulfate strongly modify the rheology of the systems. At the same time, the addition of the other halides to GG and SH does not affect significantly the values of $\eta_0$ and $\lambda$.

A further peculiar case concerns the three phosphate anions (Fig. 5). In fact, the rheological profiles show that $HPO_4^{2-}$ increases the viscosity of the SH solution to 77.68 Pa·s, while $H_2PO_4^-$ lowers (19.75) and $PO_4^{3-}$ dramatically breaks down the flow curves.

We recall that the rheological properties of hyaluronate strongly depend on the pH in a non-linear correlation (Gatej, Popa, & Rinaudo, 2005; Gibbs, Merrill, & Smith, 1968; Gura, Hückel, & Müller, 2003; Maleki, Kjøniksen, & Nyström, 2008). In particular for hyaluronic acid the complex viscosity reaches a maximum value at about pH = 2.5, sided by two remarkable drops in acid (pH = 1.6) and mid-acid conditions (pH = 3.34) (Gatej et al., 2005). The stiffening of the hyaluronic network is attributed to a critical balance between attractive and repulsive forces. These forces that involve ionized or neutral carboxylic and amino groups are mainly electrostatic (Gibbs et al., 1968). Moreover, above pH = 12 the viscosity dramatically breaks down, leading to a Newtonian-like behavior. Finally, in a wide range of pH (between 2.8 and 12) the rheological properties and viscosity remain unchanged (Gatej et al., 2005; Maleki, 2008). Furthermore, Maleki investigated the dilute (0.05% w/w) and semi-dilute (0.5% w/w) regimes of HA solutions, with the pH set between 1 and 13 by adding 0.1 M phosphate buffers (Maleki et al., 2008). The results show that the presence of these buffers does not affect the pH responsivity.

The 0.5 M $Na_3PO_4$ solution provides an extremely high pH (13) that can at least partly deprotonate the —OH groups of the hyaluronate chain, breaking the cooperative HB network of the polysaccharide chains. On the other hand, our results for 0.5 M $NaH_2PO_4$ and $Na_2HPO_4$ solutions (pH = 4.7 and 9.9, respectively) differ from those reported in the literature. Presumably in these pH conditions mono-hydrogenphosphate acts as a soft cross-linker, strengthening the HB network and increasing the viscosity. We argue that the increment in viscosity is due to a combination of two cooperating effects: the basic pH promotes the deprotonation, enhancing the HB network, and at the same time the higher SH concentrations shrink the polysaccharide network where $HPO_4^{2-}$ anions bridge different chains and re-enforce the HB network.

In the presence of di-hydrogenphosphate the pH is lower. The mid-acid environment weakens the network by reducing the number of active sites available for HB. Moreover, in $H_2PO_4^-$ the number of acceptor sites for hydrogen bonding is reduced and thus the ion contribution to the strengthening of the system is reduced.

Moreover, the power law index parameter $n$ reflects how the systems respond to an applied stress. Indeed, both GG dispersions and

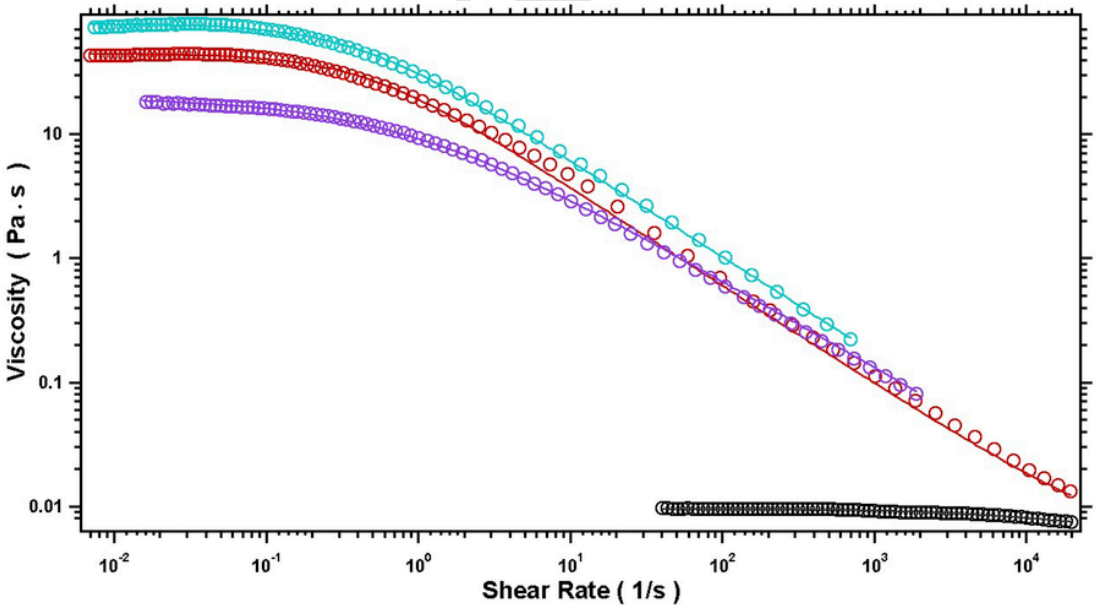


**Fig. 5.** Flow curves of SH 1% w/w pure solution (red), in the presence of 0.5 M $NaH_2PO_4$ (violet), $Na_2HPO_4$ (turquoise) and $Na_3PO_4$ (black). The solid lines represent the fitting of the experimental curves. (For interpretation of the references to colour in this figure legend, the reader is referred to the web version of this article.)

SH solutions exhibit only small fluctuations of $n$ around the value of 0.2 for all samples. Thus, the scalar law that describes the shear thinning behavior above the $\lambda$ critical value, is almost independent on the chemical nature of the added salt. After the disruption of the HB network in both cases we observed the same shear thinning effect.

In order to correlate the rheological and thermal behaviors to the thermodynamic properties of the investigated salts, we report in Fig. 6 the viscosities for GG, SH and water (on the left) and the $T_{mb}$ values for GG and SH (on the right) in the presence of $Na_2SO_4$, NaF, NaCl, NaBr, NaSCN, NaI, $NaClO_4$ as functions of the $\Delta G_{hydration}$ of the anion.

The viscosity values of aqueous salt solutions and $\Delta G_{hydration}$ are taken from literature and reported in Table S2 in the Supplementary Material (Abdulagatova et al., 2005; Goldsack & Franchetto, 1977; Galmarini et al., 2011; Hood, 1933; Janz et al., 1969; Marcus, 1991; Wolf, 1966). In the case of $T_{mb}$, the samples containing $Na_2SO_4$, NaSCN and $NaClO_4$ (only for GG) are not reported since no bound freezable water melting peak was detected in the DSC thermograms.

The viscosity plot (left panel in Fig. 6) shows that the addition of a salt to GG (black) and to water (red) produces a similar trend, in agreement to the direct Hofmeister sequence: $Na_2SO_4$ > NaF > NaCl > NaBr > NaSCN > NaI > $NaClO_4$. Thus, we conclude that the addition of a salt induces a similar modification in the viscosity for both pure water and GG dispersion. On the other hand, the trend recorded for SH differs remarkably, showing the opposite behavior and following a reverse Hofmeister series.

The added salt produces an identical effect on the $T_{mb}$ for the two polysaccharides, resulting in a decrease of the freezable bound water melting temperature moving along the series: NaF > NaCl > NaBr > NaI > $NaClO_4$.

These results confirm that the salt affects in the same way the hydration of the GG and SH by modifying the interactions between the water molecules and the polysaccharides, regardless of the different charge of their chains. Despite this, the GG dispersions and SH solutions show a diametrically opposite trend in terms of viscosities.

Kosmostropic anions induce a partial de-hydration of the polysaccharide chains, while the less hydrated chaotropic ions adsorb to the polymer chains, promote their unfolding and enhance the polymer–water interactions. The magnitude of the anion effect, both on the thermal and the rheological behaviors, is considerably higher in the case of the kosmotropic ions, whereas in the presence of chaotropic ions the behaviors are practically the same as those of the pure polysaccharide solutions.

These findings apparently point out that the degree of hydration of the polymer chains is the crucial factor that leads to a significant variation in the strength of the polysaccharide network, and that this phenomenon is ion specific. In the case of a neutral polysaccharide (guar gum) the decrease in the number of the water molecules that interact with the polysaccharide chains leads to a strengthening of the network, due to stronger inter-chain interactions. Vice versa, for a charged polysaccharide (sodium hyaluronate), electrostatic repulsive forces come into play with a greater impact, as a result of the reduced number of water molecules that can screen the charges. The overall effect is a weakening of the chain–chain interactions and, consequently the softening of the network.

## 5. Conclusions

The thermal and rheological behavior of 1% aqueous mixtures of guar gum (GG), sodium hyaluronate (SH) and sodium alginate (SA) were investigated in the presence of different salts or neutral co-solutes at constant concentration. The results suggest that the added solutes can remarkably modify the texture of the polysaccharide network by perturbing the hydration of the chains and changing their intermolecular interactions. The effect of the ions is apparently related to their hydration properties and their propensity to adsorb at the polymer interface. As a matter of fact a strongly hydrated (kosmotropic) ion is expected to deprive the polysaccharide chain of water, remain confined in the bulk solution, and enhance the interchain interaction in the case of the neutral GG. This results in a remarkable strenghtening of the system. On the other hand with the negatively charged SH, kosmotropes induce a weakening in the interactions. The chaotropes (bromide, iodide, thiocyanate) do not change the rheological properties of the mixtures. Being almost unhydrated, these ions are assumed to adsorb at the polymer surface and partially deplete some water from the hydration layer. This phenomenon is supposed to favor the unfolding of the chain, increase its hydration and reduce the interchain interactions. Phosphate ions deserve a special comment, in fact $PO_4^{3-}$ and $H_2PO_4^-$ lower the viscosity, while $HPO_4^{2-}$ produces a significant increment in the viscosity, both for GG and SH. Such behavior is probably related to a delicate balance between the different pH properties and the capacity of the three ions to strengthen the HB network.

These results are relevant for the formulation of greener frac fluids to be used in shale gas exploitation. More work is necessary to modify the behavior of more diluted polysaccharide solutions and dispersions (e.g. 0.5%), to study the effect of more concentrated salt solutions, to check the effect of temperature and pressure, and of other physico-chemical triggers for controlling the viscosity of the frac fluid in the different stages of the life of a basin.

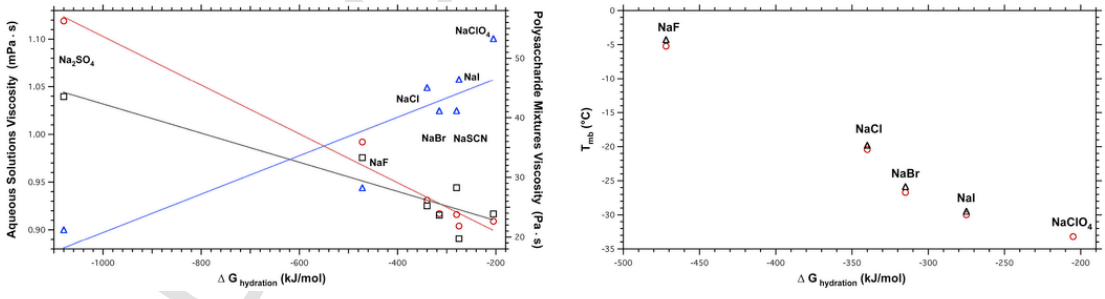


**Fig. 6.** Left panel: viscosity values for GG (black), SH (blue) and water (red) in the presence of the different sodium salts as a function of the $\Delta G_{hydration}$ of the anion. The left axis refers to the red line, while the right axis refers to black and blue lines. The dotted lines are only a guide for the eye. Right panel: $T_{mb}$ for GG (black) and SH (red) in the presence of different sodium salts as a function of the $\Delta G_{hydration}$ of the anion. (For interpretation of the references to colour in this figure legend, the reader is referred to the web version of this article.)

## Uncited references

Gosh et al. (1993), Lo Nostro et al. (2010), Morris et al. (1980), Sawayama and Kawabata (1991), Sasaki (2002), Scott and Tigwell (1975), Scott and Tigwell (1977), Setschenow (1889), Sheehan et al. (1977) and Yudianti et al. (2015).

## Acknowledgments

The authors acknowledge funding from the European Union Horizon 2020 research and innovation programme under grant agreement No. 640979.

## Appendix A. Supplementary data

Supplementary data associated with this article can be found, in the online version, at http://dx.doi.org/10.1016/j.carbpol.2017.05.078.

## References

Anghel, E.M., Georgiev, A., Petrescu, S., Popov, R., Constantinescu, M., 2014. Thermo-physical characterization of some paraffins used as phase change materials for thermal energy storage. Journal of Thermal Analysis and Calorimetry 117, 557–566.

Arakawa, T., Timasheff, S.N., 1982. Preferential interactions of proteins with salts in concentrated solutions. Biochemistry 21, 6545–6552.

Arthur, J.D., Bohm, B.K., Coughlin, B.J., Layne, M.A., Cornue, D., 2009. Evaluating the environmental implications of hydraulic fracturing in shale gas reservoirs. Society of Petroleum Engineers 121038, 1–15.

Barati, R., Liang, J.-T., 2014. A review of fracturing fluid systems used for hydraulic fracturing of oil and gas wells. Journal of Applied Polymer Science 131 (16).

Barnes, H.A., Hutton, J.F., Walters, K., 1989. An introduction to rheology. Elsevier.

Branca, C., Maccarrone, S., Magazù, S., Maisano, G., Bennington, S.M., Taylor, J., 2005. Tetrahedral order in homologous disaccharide-water mixtures. The Journal of Chemical Physics 122, 174513.

Carreau, P.J., 1972. Rheological equations from molecular network theories. Journal of Rheology 16 (1), 99–127.

Chaplin, M. (n.d.). *Polysaccharide hydration*. Retrieved March 16, 2017, from http://www1.lsbu.ac.uk/water/polysaccharide_hydration.html.

Collins, K.D., 2004. Ions from the Hofmeister series and osmolytes: Effects on proteins in solution and in the crystallization process. Methods 34, 300–311.

Couillet, I., & Hughes, T. (2008). Aqueous fracturing fluid. US Patent 7,427,583B2, Retrieved: March 16, 2017.

Curtis, R.A., Steinbrecher, C., Heinemann, M., Blanch, H.W., Prausnitz, J.M., 2002. Hydrophobic forces between protein molecules in aqueous solutions of concentrated electrolyte. Biophysical Chemistry 98 (3), 249–265.

De Andres-Santos, A.I., Velasco-Martin, A., Hernández-Velasco, E., Martín-Gil, J., Martín-Gil, F.J., 1994. Thermal behaviour of aqueous solutions of sodium hyaluronate from different commercial sources. Thermochimica Acta 242, 153–160.

Elsabee, M., Prankerd, R.J., 1992. Solid-state properties of drugs. II: Peak shape analysis and deconvolution of overlapping endotherms in differential scanning calorimetry of chiral mixtures. International Journal of Pharmaceutics 86, 211–219.

Escudier, M.P., Gouldson, I.W., Pereira, A.S., Pinho, F.T., Poole, R.J., 2001. On the reproducibility of the rheology of shear-thinning liquids. Journal of Non-Newtonian Fluid Mechanics 97, 99–124.

Escudier, M.P., Poole, R.J., Presti, F., Dales, C., Nouar, C., Desaubry, C., et al., 2005. Observations of asymmetrical flow behaviour in transitional pipe flow of yield-stress and other shear-thinning liquids. Journal of Non-Newtonian Fluid Mechanics 127, 143–155.

Gandossi, L., Von Estorff, U., 2015. An overview of hydraulic fracturing and other formation stimulation technologies for shale gas production—Update 2015. JRC technical report. EUR 26347.

García, C., Alfaro, C., Calero, N., Muñoz, J., 2014. Influence of polysaccharides on the rheology and stabilization of α-pinene emulsions. Carbohydrate Polymers 105, 177–183.

Gatej, I., Popa, M., Rinaudo, M., 2005. Role of the pH on hyaluronan behavior in aqueous solution. Biomacromolecules 6, 61–67.

Gibbs, D.A., Merrill, E.W., Smith, K.A., 1968. Rheology of hyaluronic acid. Biopolymers 6, 777–791.

Goel, N., Shah, S.N., Grady, B.P., 2002. Correlating viscoelastic measurements of fracturing fluid to particles suspension and solids transport. Journal of Petroleum Science and Engineering 35 (1–2), 59–81.

Gosh, S., Kobal, I., Zanette, D., Reed, W.F., 1993. Conformational contraction and hydrolysis of hyaluronate in sodium hydroxide solutions. Macromolecules 26, 4685–4693.

Guan, L., Xu, H., Huang, D., 2010. The investigation on states of water in different hydrophilic polymers by DSC and FTIR. Journal of Polymer Research 18, 681–689.

Gura, E., Hückel, M., Müller, P.-J., 2003. Specific degradation of hyaluronic acid and its rheological properties. Polymer Degradation and Stability 59, 297–302.

Hall, B.E., Szemenyei, C.A., Gupta, D.V.S., 1991. Breaker system for aqueous fluids containing xanthan gums. Retrieved: March 16, 2017, from http://www.google.ch/patents/US5054552.

Hatakeyama, T., Naoi, S., Hatakeyama, H., 2004. Liquid crystallization of glassy guar gum with water. Thermochimica Acta 416, 121–127.

Hatakeyama, T., Tanaka, M., Hatakeyama, H., 2010. Thermal properties of freezing bound water restrained by polysaccharides. Journal of Biomaterials Science, Polymer Edition 21, 1865–1875.

Haward, S.J., Jaishankar, A., Oliveira, M.S.N., Alves, M.A., McKinley, G.H., 2013. Extensional flow of hyaluronic acid solutions in an optimized microfluidic cross-slot device. Biomicrofluidics 7 (4).

Holloway, M.D., Rudd, O., 2013. Fracking: The operations and environmental consequences of hydraulic fracturing. John Wiley & Sons.

Jain and Roy, 2008 K.N. Jain, I. Roy, Effect of trehalose on protein structure, Protein Science 18 (2008) 24–36.

Kawai, H., Sakurai, M., Inoue, Y., Chujo, R., Kobayashi, S., 1992. Hydration of oligosaccharides: Anomalous hydration ability of trehalose. Cryobiology 29, 599–606.

Kelly, R.M., Khan, S.A., Leduc, P., Tayal, A., Prud'homme, R.K., 2001. Methods and compositions for fracturing subterranean formations. Retrieved: March 16, 2017, from http://www.google.com/patents/US5421412.

Kupská, I., Lapcík, L., Lapcíková, B., Záková, K., Juríková, J., 2014. The viscometric behaviour of sodium hyaluronate in aqueous and KCl solutions. Colloids and Surfaces A: Physicochemical and Engineering Aspects 454, 32–37.

López-Arenas, L., Solís-Mendiola, S., Padilla-Zúñiga, J., Hernández-Arana, A., 2006. Hofmeister effects in protein unfolding kinetics: Estimation of changes in surface area upon formation of the transition state. Biochimica Et Biophysica Acta (BBA): Proteins and Proteomics 1764, 1260–1267.

Legemah, M., Qu, Q., Sun, H., Beall, B., Zhou, J., 2013. Alternative polysaccharide fracturing fluids for harsh reservoir conditions. Presented at the SPE unconventional resources conference and exhibition-Asia pacific, society of petroleum engineers

Lerbret, A., Bordat, P., Affouard, F., Guinet, Y., Hedoux, A., Paccou, L., et al., 2005. Influence of homologous disaccharides on the hydrogen-bond network of water: complementary Raman scattering experiments and molecular dynamics simulations. Carbohydrate Research 340, 881–887.

Lertwimolnun, W., Vergnes, B., 2006. Effect of processing conditions on the formation of polypropylene/organoclay nanocomposites in a twin screw extruder. Polymer Engineering and Science 46, 314–323.

Li, L., Al-Muntasheri, G.A., Liang, F., 2016. A review of crosslinked fracturing fluids prepared with produced water. Petroleum 2 (4), 313–323.

Lo Nostro, P., Ninham, B.W., 2012. Hofmeister phenomena: An update on ion specificity in biology. Chemical Reviews 112, 2286–2322.

Lo Nostro, P., Ninham, B.W., 2016. Editorial: Electrolytes and specific ion effects. New and old horizons. Current Opinion in Colloid & Interface Science 23, A1–A5.

Lo Nostro, P., Peruzzi, N., Severi, M., Ninham, B.W., Baglioni, P., 2010. Asymmetric partitioning of anions in lysozyme dispersions. Journal of American Chemical Society 132, 6571–6577.

Magazù, S., Migliardo, P., Musolino, A.M., Sciortino, M.T., 1997. α,α-Trehalose-water solutions. 1. Hydration phenomena and anomalies in the acoustic properties. Journal Physical Chemistry B 101, 2348–2351.

Maleki, A., Kjøniksen, A.-L., Nyström, B., 2008. Effect of pH on the behavior of hyaluronic acid in dilute and semidilute aqueous solutions. Macromolecular Symposia 274, 131–140.

Marcus, Y., 1991. Thermodynamics of solvation of ions. Part 5. Gibbs free energy of hydration at 298.15 K. Journal of the Chemical Society, Faraday Transactions 87 (18), 2995–2999.

Montgomery, C., 2013. Fracturing fluid components. In: Jeffrey, R. (Ed.), Effective and sustainable hydraulic fracturing. InTech, pp. 25–45.

Morris, E.R., Rees, D.A., Welsh, E.J., 1980. Conformation and dynamic interactions in hyaluronate solutions. Journal of Molecular Biology 138, 383–400.

Nakamura, K., Hatakeyama, T., Hatakeyama, H., 1991. Formation of the liquid crystalline state in the water–sodium alginate system. Sen'i Gakkaishi 47, 421–423.

Nandhini Venugopal, K., Abhilash, M., 2010. Study of hydration kinetics and rheological behaviour of guar gum. International Journal of Pharma Sciences and Research 1 (1), 28–39.

Naoi, S., Hatakeyama, T., Hatakeyama, H., 2002. Phase transition of locust bean gum-, tara gum- and guar gum-water systems. Journal of Thermal Analysis and Calorimetry 70, 841–852.
Norton, I.T., Morris, E.R., Rees, D.A., 1984. Lyotropic effects of simple anions on the conformation and interactions of kappa-carrageenan. Carbohydrate Research 134, 89–101.
Osborn, S.G., Vengosh, A., Warner, N.R., Jackson, R.B., 2011. Methane contamination of drinking water accompanying gas-well drilling and hydraulic fracturing. Proceedings of the National Academy of Sciences 108 (20), 8172–8176.
Osswald, T., Rudolph, N., 2015. Polymer rheology. Understanding plastics rheology. Hanser.
Piculell, L., Nilsson, S., 1989. Anion-specific salt effects in aqueous agarose systems. 1. Effects on the coil-helix transition and gelation of agarose. Journal of Physical Chemistry 93, 5596–5601.
Sasaki, K., 2002. Charge screening effect in metallic carbon nanotubes. Physical Review B 65, 195412.
Sawayama, S., Kawabata, A., 1991. Effect of salts on the thermal properties of pectin solution on freezing and thawing. Food Hydrocolloids 5, 393–405.
Schnoor, E.A., Singh, D., Russel, A.G., 2016. Aldehydes as a catalyst for an oxidative breaker. Retrieved: March 16, 2017, from http://www.google.it/patents/WO2016099502A1.
Schultheiss, N.C., 2015. Multi-component materials for breaker activity control. Retrieved: March 16, 2017, from http://www.google.it/patents/WO2015020670A1.
Schwierz, N., Horinek, D., Sivan, U., Netz, R.R., 2016. Reversed Hofmeister series—The rule rather than the exception. Current Opinion in Colloid & Interface Science 23, 10–18.
Scott, J.E., Tigwell, M.J., 1975. The influence of the intrapolymer environment on periodate oxidation of uronic acids in polyuronides and glycosaminoglycuronans. Biochemical Society Transactions 3, 662–664.
Scott, J.E., Tigwell, M.J., 1977. Periodate oxidation and the shapes of glycosaminoglycuronans in solutions. Biochemical Journal 173, 103–114.
Setschenow, J., 1889. Über die konstitution der salzlösungen auf grund ihres verhaltens zu kohlensäure. Zeitschrift fur Physikalische Chemie 4, 117–125.
Sheehan, J.K., Gardner, K.H., Atkins, E.D.T., 1977. Hyaluronic acid: A double-helical structure in the presence of potassium at low pH and found also with the cations ammonium, rubidium and caesium. Journal of Molecular Biology 117, 113–135.
Singh, T., Meena, R., Kumar, A., 2009. Effect of sodium sulfate on the gelling behavior of agarose and water structure inside the gel networks. Journal of Physical Chemistry B 113, 2519–2525.
Tatini, D., Tempesti, P., Ridi, F., Fratini, E., Bonini, M., Baglioni, P., 2015. Pluronic/gelatin composites for controlled release of actives. Colloids and Surfaces B: Biointerfaces 135, 400–407.
Vengosh, A., Jackson, R.B., Warner, N., Darrah, T.H., Kondash, A., 2014. A critical review of the risks to water resources from unconventional shale gas development and hydraulic fracturing in the United States. Environmental Science & Technology 48 (15), 8334–8348.
Winkworth-Smith, C.G., MacNaughtan, W., Foster, T.J., 2016. Polysaccharide structures and interactions in a lithium chloride/urea/water solvent. Carbohydrate Polymers 149, 231–241.
Xu, Y., Wang, C., Tam, K.C., Li, L., 2004. Salt-assisted and salt-duppressed sol–gel transitions of methylcellulose in water. Langmuir 20, 646–652.
Yasuda, K., Armstrong, R.C., Cohen, R.E., 1981. Shear flow properties of concentrated solutions of linear and star branched polystyrenes. Rheologica Acta 20 (2), 163–178.
Yin, W., Zhang, H., Huang, L., Nishinari, K., 2008. Effects of the lyotropic series salts on the gelation of konjac glucomannan in aqueous solutions. Carbohydrate Polymers 74, 68–78.
Yudianti, R., Karina, M., Sakamoto, M., Azuma, J., 2015. DSC analysis on water state of salvia hydrogels. Macromolecular Research 17, 1015–1020.